Supplementary Materials

5-(*N*-Trifluoromethylcarboxy)aminouracil as a Potential DNA Radiosensitizer and its Radiochemical Conversion into *N*-uracil-5-yloxamic Acid

Paulina Spisz, Witold Kozak, Lidia Chomicz-Mańka, Samanta Makurat, Karina Falkiewicz, Artur Sikorski, Anna Czaja, Janusz Rak, Magdalena Zdrowowicz*

Department of Physical Chemistry, Faculty of Chemistry, University of Gdańsk, Wita Stwosza 63, 80-308 Gdańsk, Poland; paulina.rewers@phdstud.ug.edu.pl (P.S.); davelombardo@wp.pl (W.K.); lidia.chomicz-manka@ug.edu.pl (L.C-M.) samanta.makurat@ug.edu.pl (S.M.); karina.falki@gmail.com, (K.F.); artur.sikorski@ug.edu.pl (A.S.); czaja.ania@yahoo.com (A.C.); janusz.rak@ug.edu.pl (J.R.);

* Correspondence: magdalena.zdrowowicz@ug.edu.pl; (M.Z.)

Received: date; Accepted: date; Published: date

Table of Content

NMR spectra of 5-(*N*-trifluoromethylcarboxy)aminouracil

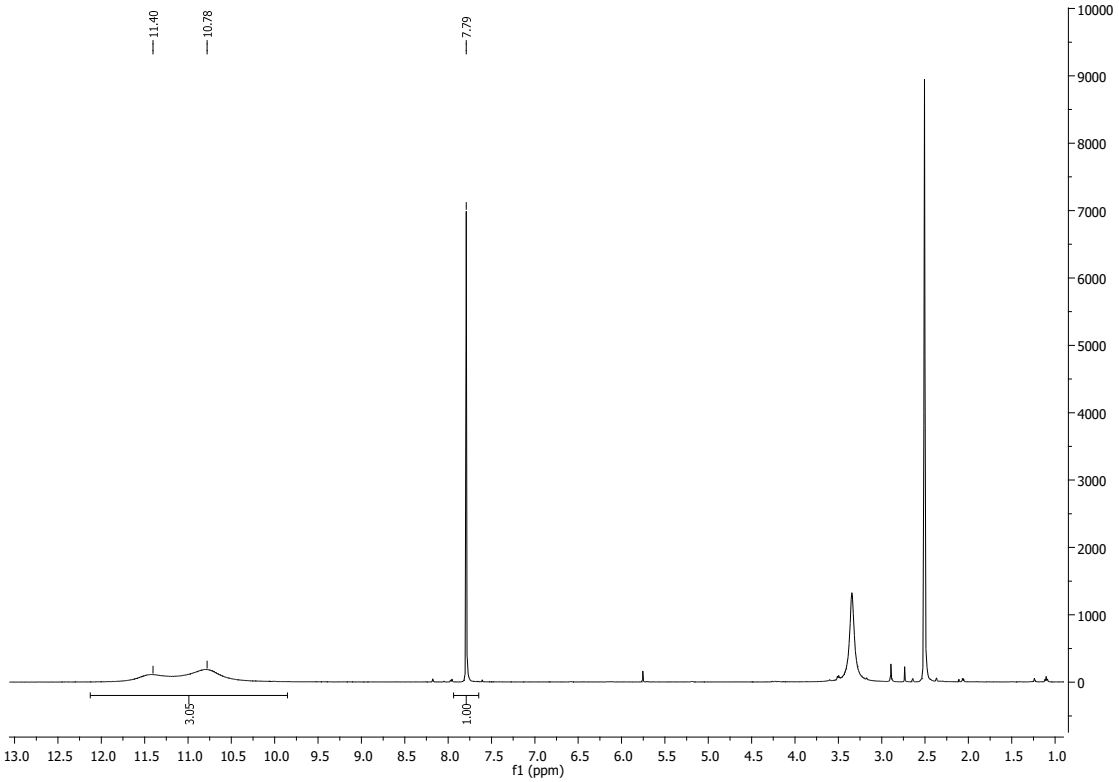

Figure S1. ^{1}H NMR spectrum of 5-(*N*-trifluoromethylcarboxy)aminouracil.

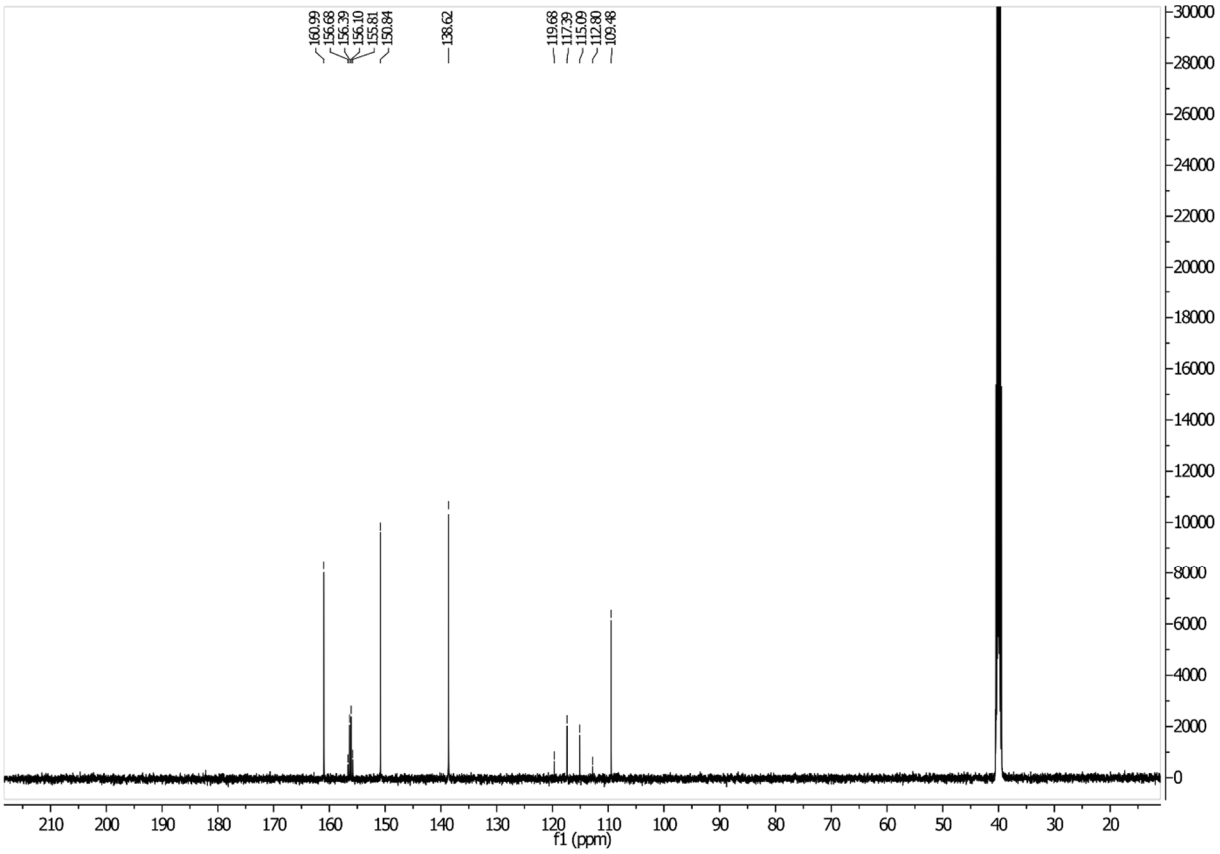

Figure S2. ^{13}C NMR spectrum of 5-(*N*-trifluoromethylcarboxy)aminouracil.

MS and MS/MS spectra of a 5-(*N*-trifluoromethylcarboxy)aminouracil

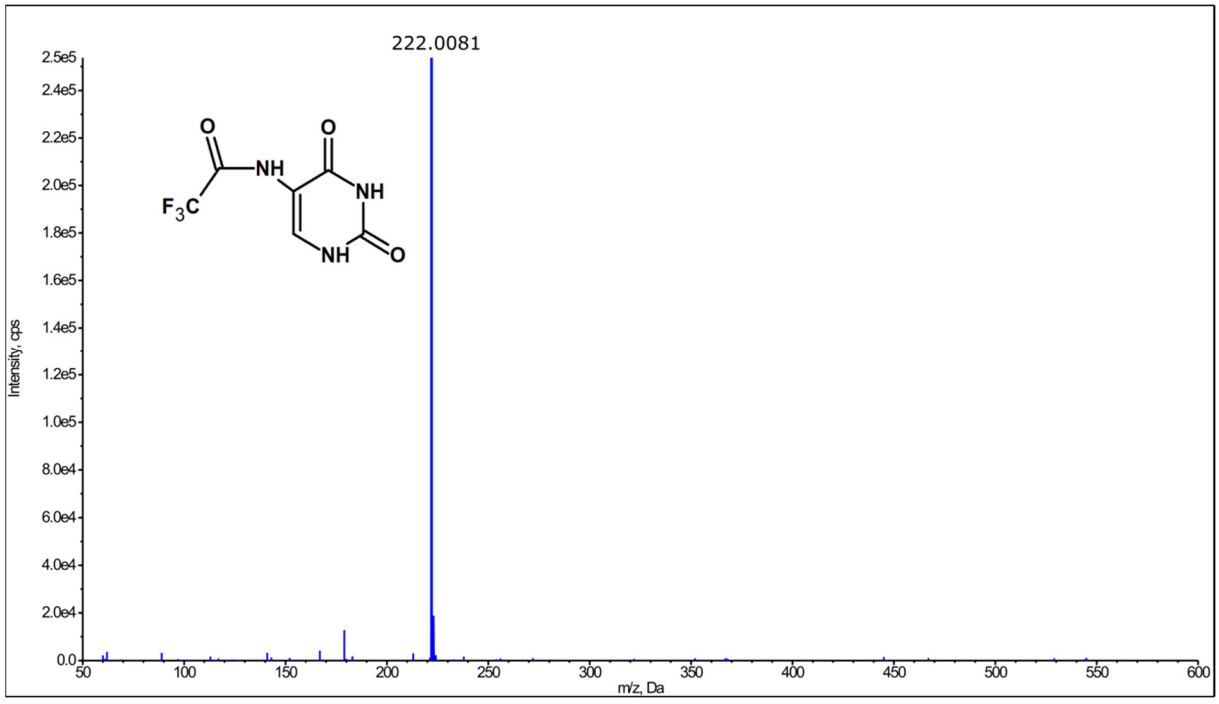

Figure S3. The MS spectrum (in negative ionization mode) of 5-(*N*-trifluoromethylcarboxy)-aminouracil.

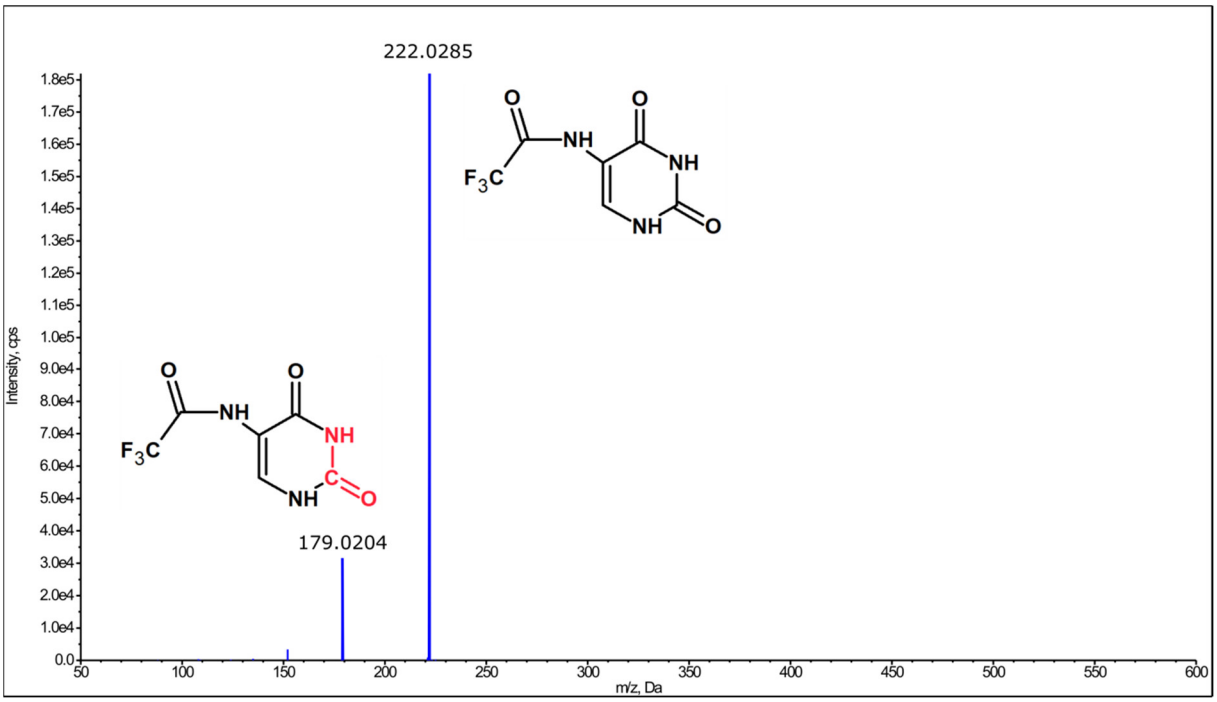

Figure S4. The MS/MS spectrum (in negative ionization mode) of 5-(*N*-trifluoromethyl-carboxy)aminouracil and ion identities.

MS and MS/MS spectra of a radioproduct

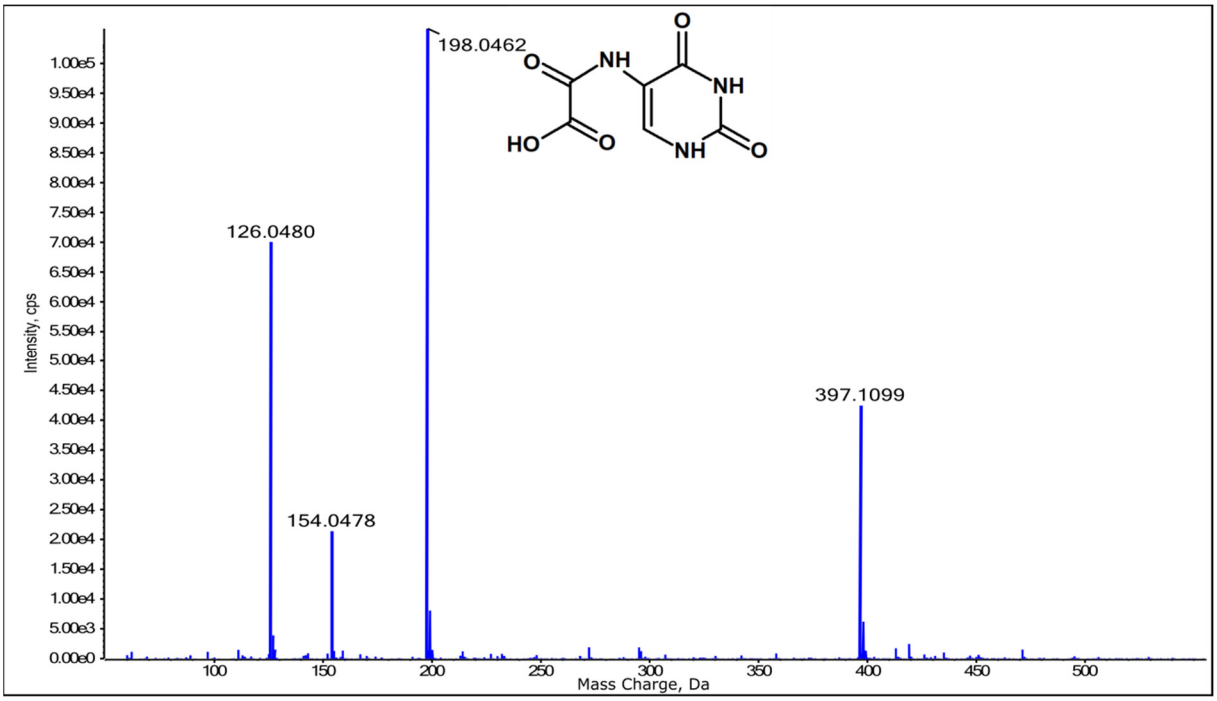

Figure S5. The MS spectrum (in negative ionization mode) of radioproduct.

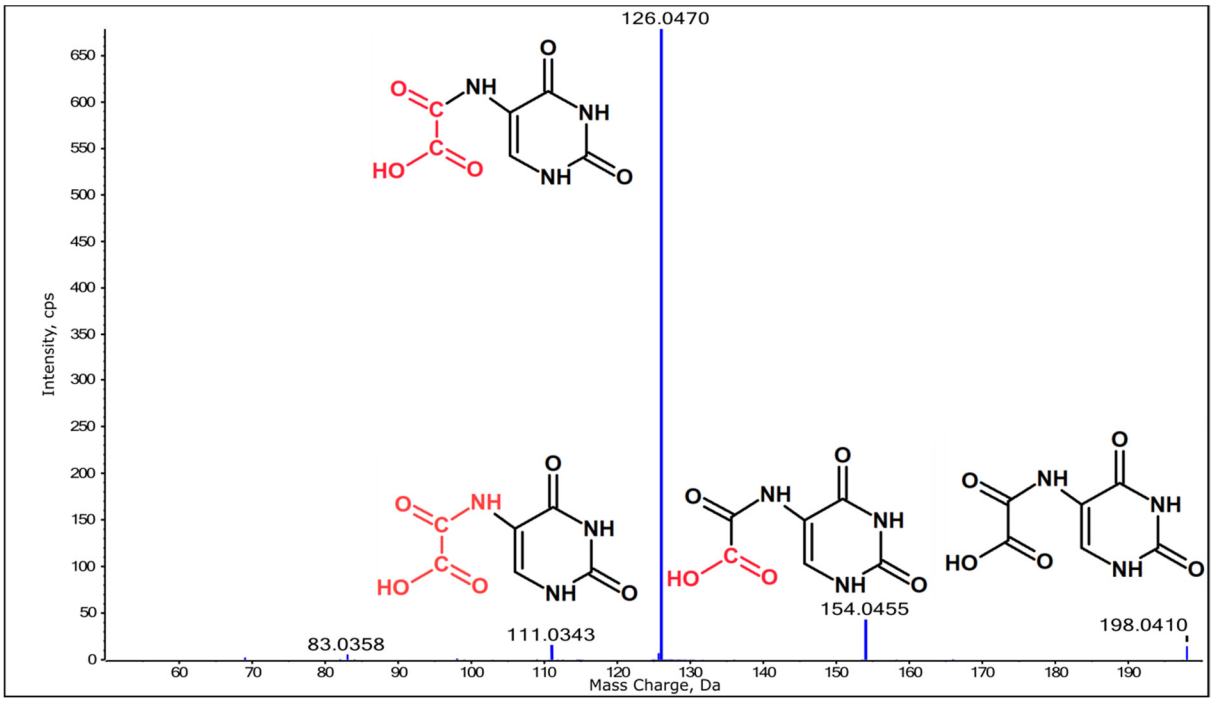

Figure S6. The MS/MS spectrum (in negative ionization mode) of radioproduct and ion identities.

Crystallographic data for 5-(*N*-trifluoromethylcarboxy)aminouracil

Table S1. Crystal data and structure refinement parameters for 5-(*N*-trifluoromethylcarboxy)aminouracil.

Chemical formula	$C_6H_4N_3F_3O_3$
FW/g · mol^{-1}	223.12
Crystal system	monoclinic
Space group	*C*2/c
a/Å	19.616(3)
b/Å	7.268(2)
c/Å	11.663(3)
α/°	90
β/°	100.55(2)
γ/°	90
V/Å^3	1634.8(6)
Z	8

T/K	295(2)
λ_{Mo}/Å	0.71073
ρ_{calc}/g·cm^{-3}	1.813
F(000)	896
μ/mm^{-1}	0.187
θ range/°	3.38–25.00
Completness θ/%	99.9
Reflections collected	5089
Reflections unique	1441 [R_{int} = 0.1635]
Data/restraints/parameters	1441/0/145
Goodness of fit on F^2	0.957
Final R_1 value (I>2σ(I))	0.0706
Final wR_2 value (I>2σ(I))	0.1259
Final R_1 value (all data)	0.1938
Final wR_2 value (all data)	0.1733
CCDC number	2016475

Table S2. Hydrogen bonding interactions in the crystal structure of the title compound.

D–H···A	*d*(D–H) (Å)	*d*(H···A) (Å)	*d*(D···A) (Å)	<D–H···A (°)
N1–H1···O7^{i}	0.99(6)	1.83(6)	2.821(6)	174(4)
N3–H3···O8^{ii}	0.77(6)	2.13(6)	2.878(6)	165(6)
N9–H9···O8^{iii}	0.86(6)	2.04(6)	2.823(6)	151(5)
C6–H6···O11^{iv}	0.93	2.58	3.284(7)	133

Symmetry codes:(i) 1/2−x,−1/2−y,1−z; (ii) 1−x,−y,1−z; (iii) 1−x,y,3/2−z; (iv) 1/2−x,−1/2+y,3/2−z.

Plating efficiencies (clonogenic assay)

Table S3. Plating efficiencies and survival fractions (obtained from clonogenic assay) for the PC3 cells treated with 5-(*N*-trifluoromethylcarboxy)aminouracil and/or radiation.

Dose [Gy]	0 μM CF_3CONHU		100 μM CF_3CONHU	
	Plating efficiency	**Survival fraction**	**Plating efficiency**	**Survival fraction**
0	40.66 ± 0.09	100.0	42.09 ± 0.22	100.0
0.5	35.06 ± 0.56	86.2 ± 2.2	28.88 ± 2.25	68.6 ± 7.1
1	28.25 ± 1.25	69.5 ± 4.1	23.81 ± 0.44	56.6 ± 1.9
2	17.63 ± 0.75	43.4 ± 2.8	13.68 ± 1.31	32.5 ± 4.6
4	4.69 ± 0.94	11.5 ± 3.2	1.75 ± 0.38	4.2 ± 1.3

Hypothetic pathway for the formation of 2-oxazolidinone ring

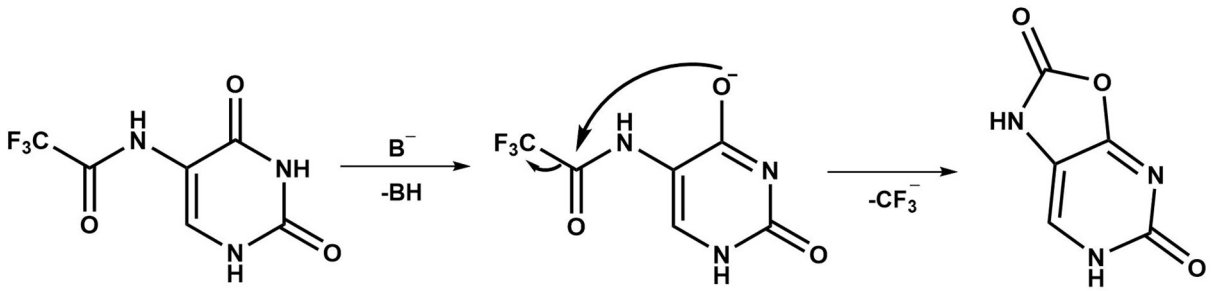

Figure S7. Hypothetic pathway for the formation of 2-oxazolidinone ring.

Kinetic model

In order to mimic the experimental conditions k_1 (Scheme S1) was assumed to be equal to $3.3 \cdot 10^{-8}$, which corresponds to the concentration of solvated electrons and hydroxyl radicals generated by the experimental dose rate ($0.117\ Gy \cdot s^{-1}$). We further assumed that the concentration of water, *t*-butanol (both used in large excess) and hydroxyl anions (the sample was buffered, see point 2.2.3 Radiolysis) was constant during the experiment and equal to 55.5, $3.0 \cdot 10^{-2}$ and $1.0 \cdot 10^{-7}$ M, respectively. For k_2 (Scheme S1), the rate reported for the reaction between e_{hyd} and pyrimidine was assumed [S1], while for k_3 (Scheme S1) the value assigned for the reaction rate between the •OH radicals and *t*-butanol, while k_6 results from the Debye equation for water and T = 298 K [S2]. Finally k_{14} (Scheme S1) was assumed to be equal to the rate evaluated by Mezyk and Madden [S3] for the self –recombination of *t*-butyl alcohol radicals in water. The remaining rate constants were obtained using transition state theory and ΔG^* calculated at the M06-2X/6-31++G(d,p) level (Figure 6). The system of differential equations (Equation S1) matching the mechanism depicted in Scheme 1 was integrated for 1200 s and then for further 60 000 s with k_1 (Scheme S1) set to 0, that corresponded to X-ray source turned off. Reactions 1, 2, 3 and 9 (Scheme S1) were assumed to be irreversible since the thermodynamic stimuli for the reverse processes were highly unfavorable (from 17.4 for reaction (3) to even 67.2 kcal $\cdot$ mol^{-1} for reaction (9)) making the reverse reactions completely improbable at the ambient temperature.

$$H_2O \xrightarrow{X,\,k_1} OH^{\bullet} + e_{sol} \quad (1)$$

$$[CF_3 - CO - R] + e_{sol} \xrightarrow{k_2} [CF_3 - CO - R]^{\bullet -} \quad (2)$$

$$[t - But] + [OH]^{\bullet} \xrightarrow{k_3} [t - But]^{\bullet} + H_2O \quad (3)$$

$$[CF_3 - CO - R]^{\bullet -} \underset{k_5}{\overset{k_4}{\rightleftarrows}} [CF_2 - CO - R]^{\bullet} + F^- \quad (4)$$

$$[CF_2 - CO - R]^{\bullet} + OH^- \underset{k_7}{\overset{k_6}{\rightleftarrows}} [CF_2OH - CO - R]^{\bullet -} \quad (5)$$

$$[CF_2OH - CO - R]^{\bullet -} \underset{k_9}{\overset{k_8}{\rightleftarrows}} [CFOH - CO - R]^{\bullet} + F^- \quad (6)$$

$$[CFOH - CO - R]^{\bullet} + H_2O \underset{k_{11}}{\overset{k_{10}}{\rightleftarrows}} [CO - CO - R]^{\bullet} + H_2O + HF \quad (7)$$

$$[CO - CO - R]^{\bullet} + H_2O \underset{k_{13}}{\overset{k_{12}}{\rightleftarrows}} [COOH - COH - R]^{\bullet} \quad (8)$$

$$[COOH - COH - R]^{\bullet} + [t - But]^{\bullet} \xrightarrow{k_{14}} [COOH - CO - R] + [t - But] \quad (9)$$

Scheme S1. Elementary reactions leading from the radical anion of CF_3CONHU to *N*-uracil-5-yloxamic acid. R = NHU.

Equation S1. System of kinetic equations used for predicting the time of reaction completion.

$$1)\ \frac{d[e_{sol}]}{dt} = k_1 - k_2[CF_3 - CO - R][e_{sol}]$$

$$2)\ \frac{d[OH]^{\bullet}}{dt} = k_1 - k_3[OH]^{\bullet}[t - But]$$

$$3)\ \frac{d[CF_3 - CO - R]^{\bullet -}}{dt} = -k_4[CF_3 - CO - R]^{\bullet -} + k_5[CF_2 - CO - R]^{\bullet}[F^-] + k_2\,[CF_3 - CO - R][e_{sol}]$$

$$4)\ \frac{d[CF_2 - CO - R]^{\bullet}}{dt} = -k_6[CF_2 - CO - R]^{\bullet}[OH^-] + k_7[CF_2OH - CO - R]^{\bullet -} - k_5[CF_2 - CO - R]^{\bullet}[F^-] + k_4[CF_3 - CO - R]^{\bullet -}$$

$$5)\ \frac{d\,[CF_2OH - CO - R]^{\bullet -}}{dt} = -k_8\,[CF_2OH - CO - R]^{\bullet -} + k_9\,[CFOH - CO - R]^{\bullet}\,[F^-] - k_7[CF_2OH - CO - R]^{\bullet -} + k_6[CF_2 - CO - R]^{\bullet}[OH^-]$$

$$6)\ \frac{d[CFOH - CO - R]^{\bullet}}{dt} = -k_{10}[CFOH - CO - R]^{\bullet}[H_2O] + k_{11}[CO - CO - R]^{\bullet}[H_2O][HF] - k_9[CFOH - CO - R]^{\bullet}[F^-] + k_8[CF_2OH - CO - R]^{\bullet -}$$

$$7)\ \frac{d[F^-]}{dt} = k_4[CF_3 - CO - R]^{\bullet -} - k_5[CF_2 - CO - R]^{\bullet}[F^-] + k_8\,[CF_2OH - CO - R]^{\bullet -} - k_9\,[CFOH - CO - R]^{\bullet}\,[F^-]$$

$$8)\ \frac{d[CO - CO - R]^{\bullet}}{dt} = -k_{12}[CO - CO - R]^{\bullet}[H_2O] + k_{13}[COOH - COH - R]^{\bullet} - k_{11}[CO - CO - R]^{\bullet}[H_2O][HF] + k_{10}[CFOH - CO - R]^{\bullet}[H_2O]$$

$$9)\ \frac{d[HF]}{dt} = k_{10}[CFOH - CO - R]^{\bullet}[H_2O] - k_{11}[CO - CO - R]^{\bullet}[H_2O][HF]$$

$$10)\ \frac{d\,[COOH - COH - R]^{\bullet}}{dt} = -k_{13}\,[COOH - COH - R]^{\bullet} + k_{12}[CO - CO - R]^{\bullet}[H_2O] - k_{14}[COOH - COH - R]^{\bullet}[t - But]^{\bullet}$$

$$11)\ \frac{d\,[COOH - CO - R]}{dt} = k_{14}\,[COOH - COH - R]^{\bullet}[t - But]^{\bullet}$$

$$12)\ \frac{d\,[CF_3 - COR]}{dt} = -k_2\,[CF_3 - CO - R][e_{sol}]$$

$$13)\ \frac{d\,[t - But]^{\bullet}}{dt} = k_3[t - But][OH]^{\bullet} - k_{14}\,[COOH - COH - R]^{\bullet}[t - But]^{\bullet}$$

Table S4. Rate constants (T = 298 K) employed in the kinetic model shown in Scheme S1. The values of particular constants were obtained using transition state theory and activation free energies (ΔG^{*}) calculated at the M06-2X/6-31++G(d,p) level. [$^{-}$OH], [H_2O] and [*t*-butanol] equal to 10^{-7}, 55.5 and $3 \cdot 10^{-2}$ M, respectively.

Constant (**Scheme S1**)	kT/h*exp(-ΔG^{*}/(RT))	Invariant concentration species	Rate constant used in the kinetic calculations (**Equation S1**)
k_1	$3.3 \cdot 10^{-8}$ [M s^{-1}]		$3.3 \cdot 10^{-8}$ [M s^{-1}]
k_2 [S1]	$2.0 \cdot 10^{10}$ [M^{-1} s^{-1}]		$2.0 \cdot 10^{10}$ [M^{-1} s^{-1}]
k_3 [S4]	$6.0 \cdot 10^{8}$ [M^{-1} s^{-1}]		$6.0 \cdot 10^{8}$ [M^{-1} s^{-1}]
k_4	$5.07 \cdot 10^{5}$ [s^{-1}]		$5.07 \cdot 10^{5}$ [s^{-1}]
k_5	$3.36 \cdot 10^{12}$ [M^{-1} s^{-1}]		$3.36 \cdot 10^{12}$ [M^{-1} s^{-1}]
k_6 [S2]	$7.4 \cdot 10^{9}$ [M^{-1} s^{-1}]	$^{-}$OH	$7.4 \cdot 10^{2}$ [s^{-1}]
k_7	$1.23 \cdot 10^{-18}$ [s^{-1}]		$1.23 \cdot 10^{-18}$ [s^{-1}]
k_8	$9.38 \cdot 10^{4}$ [s^{-1}]		$9.38 \cdot 10^{4}$ [s^{-1}]
k_9	$1.20 \cdot 10^{9}$ [M^{-1} s^{-1}]		$1.20 \cdot 10^{9}$ [s^{-1}]
k_{10}	$5.99 \cdot 10^{6}$ [M^{-3} s^{-1}]	H_2O	$3.27 \cdot 10^{-4}$ [M^{-2} s^{-1}]
k_{11}	$1.03 \cdot 10^{1}$ [M^{-2} s^{-1}]	H_2O	$5.72 \cdot 10^{2}$ [M^{-1} s^{-1}]
k_{12}	$1.84 \cdot 10^{5}$ [M^{-1} s^{-1}]	H_2O	$1.02 \cdot 10^{7}$ [s^{-1}]
k_{13}	$1.53 \cdot 10^{-9}$ [s^{-1}]		$1.53 \cdot 10^{-9}$ [s^{-1}]
k_{14} [S3]	$1.20 \cdot 10^{9}$ [M^{-1} s^{-1}]	*t*-butanol	$3.6 \cdot 10^{7}$ [M^{-1} s^{-1}]

Cytometric analysis of histone H2A.X phosphorylation

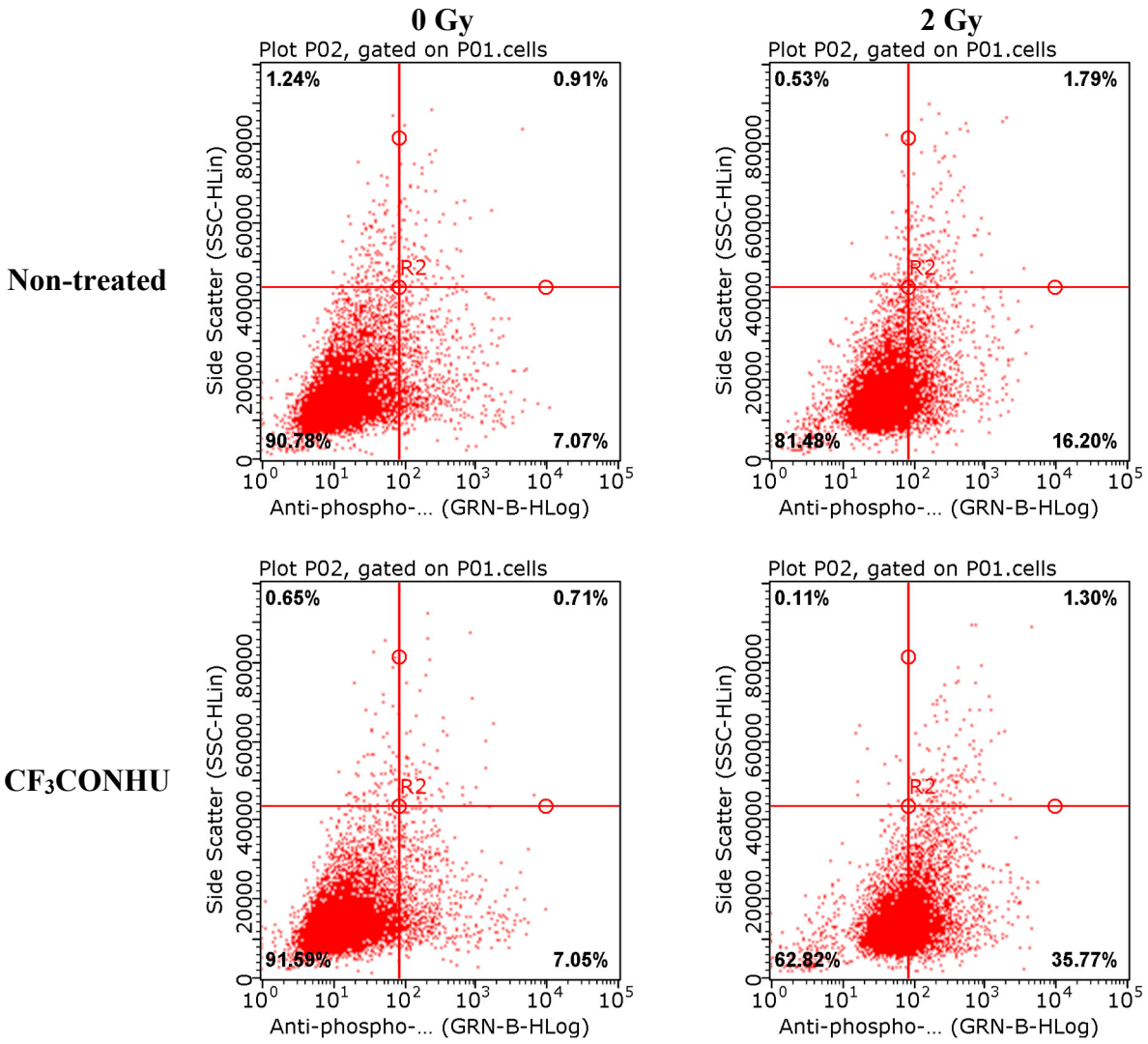

Figure S8. Flow cytometric analysis of H2A.X phosphorylation. γH2A.X was measured 1 h after irradiation.

Cytotoxicity assay

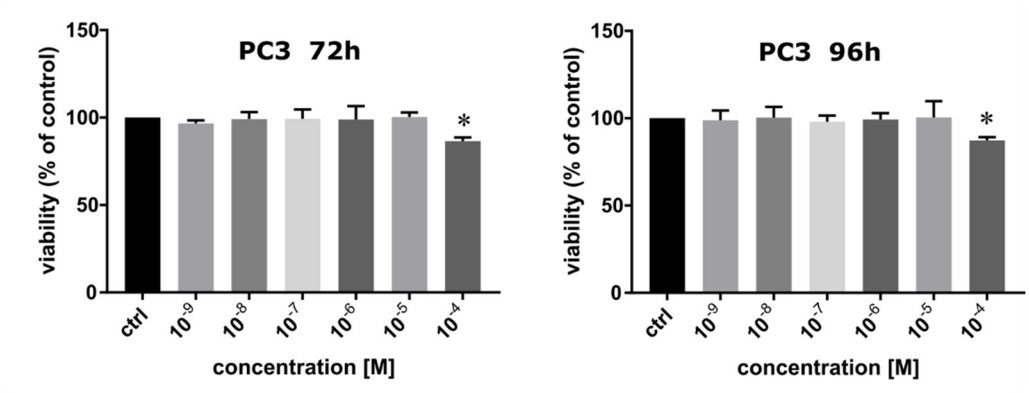

Figure S9. The viability of PC3 cells after 72 and 96 h treatment with 5-(*N*-trifluoromethylcarboxy)aminouracil in a range of concentrations from 0 to 10^{-4} M. Results are shown as mean ± SD of three independent experiments performed in triplicate.
*statistically significant difference is present between treated culture compared with control (untreated culture)

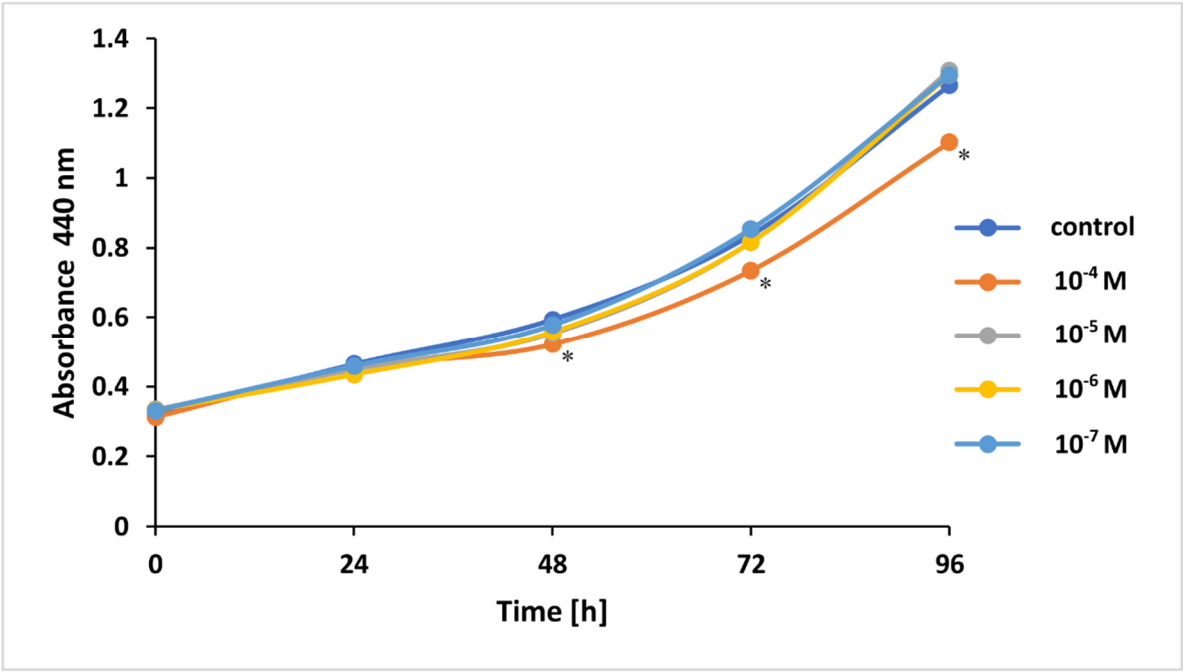

Figure S10. Cell proliferation measured using WST-1 assay. The absorbance at 440 nm plotted as a function of time.
*statistically significant difference is present between treated culture compared with control (untreated culture)

References

S1. Steenken, S. Purine bases, nucleosides, and nucleotides: aqueous solution redox chemistry and transformation reactions of their radical cations and e- and OH adducts. *Chem. Rev.* **1989**, *89*, 503–520.
S2. Debye, P. Reaction rates in ionic solutions. *Trans. Electrochem. Soc.* **1942**, *82*, 265–272.
S3. Mezyk S.P.; Madden, K.P. Self-recombination rate constants for 2-propanol and tert-butyl alcohol radicals in water. *J. Phys. Chem. A* **1999**, *103*, 235–242.
S4. Buxton, G.V.; Greenstock, C.L.; Helman, W.P.; Ross, A.B. Critical review of rate constants for reactions of hydrated electrons, hydrogen atoms and hydroxyl radicals ($^{\bullet}OH/^{\bullet}O^{-}$) in aqueous solution. *J. Phys. Chem. Ref. Data* **1988**, *17*, 513–886.